Synthesis, Structural Characterization, and Reactivity of Rare-Earth Complexes Derived from A New Phosphorus-Bridged Versatile Ligand, $^{i}Pr_2NP(C_9H_7)(C_2B_{10}H_{11})$

Hong Wang, Haiping Wang, Hung-Wing Li, and Zuowei Xie*

Department of Chemistry, The Chinese University of Hong Kong, Shatin, New Territories, Hong Kong, China

Received October 29, 2003

New phosphorus-bridged ligands incorporating both indenyl and carboranyl moieties were prepared. Reaction of $^{i}Pr_2NP(C_9H_7)Cl$ (**1**) with 1 equiv of $Li_2C_2B_{10}H_{10}$ gave, after treatment with 1 equiv of *n*-BuLi, the dilithium salt $[^{i}Pr_2NP(C_9H_6)(C_2B_{10}H_{10})]Li_2(OEt_2)_{1.5}$ (**2**). **2** can be conveniently converted into its neutral counterpart $^{i}Pr_2NP(C_9H_7)(C_2B_{10}H_{11})$ (**4**) by treatment with excess dry Me_3NHCl in CH_2Cl_2. Mixing **2** and **4** in a 1:1 molar ratio afforded quantitatively the monolithium salt $[^{i}Pr_2NP(C_9H_6)(C_2B_{10}H_{11})]Li(DME)_3$ (**3**). Reaction of YbI_2 with 1 equiv of **2** gave the organoytterbium(II) complex $[\eta^5{:}\sigma\text{-}^{i}Pr_2NP(C_9H_6)(C_2B_{10}H_{10})]Yb(DME)_2$ (**5**). **5** reacted further with 1 equiv of **3** to afford the organoytterbium(III) complex $[\{\eta^5{:}\sigma\text{-}^{i}Pr_2NP(C_9H_6)(C_2B_{10}H_{10})\}_2Yb][Li(THF)_3(Et_2O)]$ (**6**). In sharp contrast, treatment of SmI_2 with 1 equiv of **2** generated the trivalent organosamarium complex $[\{\eta^5{:}\sigma\text{-}^{i}Pr_2NP(C_9H_6)(C_2B_{10}H_{10})\}_2Sm][Li(DME)_3]$ (**7**). Reaction of $LnCl_3$ with 2 equiv of **2** gave the ionic complexes $[\{\eta^5{:}\sigma\text{-}^{i}Pr_2NP(C_9H_6)(C_2B_{10}H_{10})\}_2Ln][Li(L_1)_nL_2]]$ ($L_1 = L_2 =$ DME, $n = 2$, Ln = Sm (**7**), Nd (**8**), Er (**9**); $L_1 =$ DME, $L_2 =$ THF, $n = 2$, Ln = Y (**10**)). Reaction between equimolar amounts of $LnCl_3$ and **2** resulted in the isolation of the lanthanocene chlorides $[\{[\eta^5{:}\sigma\text{-}^{i}Pr_2NP(C_9H_6)(C_2B_{10}H_{10})]LnCl\}_2(\mu\text{-}Cl)_3Li(DME)][Li(DME)_3]_2$ (Ln = Er (**11**), Y (**12**)). The chloro groups in these complexes can be replaced by other moieties. For example, reaction of **12** with 2 equiv of KCH_2Ph afforded the unexpected compound $\{[\eta^5{:}\sigma\text{-}^{i}Pr_2NP(C_9H_6)(C_2B_{10}H_{10})]_2Y\}\{(\eta^6\text{-}C_6H_5CH_3)_2K\}$ (**13**) and treatment of **12** with 2 equiv of $NaBH_4$ produced the organoyttrium hydrides $[\{\eta^5{:}\sigma\text{-}^{i}Pr_2NP(C_9H_6)(C_2B_{10}H_{10})\}Y\{(\mu\text{-}H)_3BH\}_2][Li(DME)_3]$ (**14**). All complexes were fully characterized by various spectroscopic techniques and elemental analyses. The structures of some of the compounds were further confirmed by single-crystal X-ray analyses.

Introduction

Ligand designs and modifications have played a crucial role in developing new catalysts and catalyst precursors for various chemical transformations.[1] In this connection, we have developed several carbon-, silicon-, and boron-bridged versatile ligands,[2] $Me_2A(C_5R_4H)(C_2B_{10}H_{11})$ (A = C, R = H;[3] A = Si, R = H,[4] Me[5]), $Me_2A(C_9H_6R)(C_2B_{10}H_{11})$ (A = C, R = H;[6] A = Si, R = H,[7] CH_2CH_2OMe,[8] $CH_2CH_2NMe_2$[8]), $Me_2Si(C_{13}H_9)(C_2B_{10}H_{11})$,[9] and $^{i}Pr_2NB(C_9H_7)(C_2B_{10}H_{11})$,[10] by taking advantage of unique carborane molecules, traditional cyclic π-ligands as well as bridging ligands. Our work shows that both cyclic organic groups and bridging atoms have a large influence on the properties of these ligand systems and on the resulting organometallic compounds.[2,11,12]

Recently, phosphorus-bridged ansa ligands have attracted much attention, since the phosphorus atom has a covalent radius similar to that of silicon[13] and, on the

* To whom correspondence should be addressed. Fax: (852)-26035057. Tel: (852)26096269. E-mail: zxie@cuhk.edu.hk.

(1) For reviews, see: (a) Britovsek, G. J. P.; Gibson, V. C.; Wass, D. F. *Angew. Chem., Int. Ed.* **1999**, *38*, 428. (b) Kaminsky, W.; Arndt, M. *Adv. Polym. Sci.* **1997**, *127*, 144. (c) Bochmann, M. *J. Chem. Soc., Dalton Trans.* **1996**, 255. (d) Kaminsky, W. *Macromol. Chem. Phys.* **1996**, *197*, 3907. (e) Brintzinger, H. H.; Fisher, D.; Mülhaupt, R.; Rieger, B.; Waymouth, R. M. *Angew. Chem., Int. Ed. Engl.* **1995**, *34*, 1143. (f) Möhring, R. C.; Coville, N. J. *J. Organomet. Chem.* **1994**, *479*, 1. (g) Marks, T. J. *Acc. Chem. Res.* **1992**, *25*, 57. (h) Jordan, R. F. *Adv. Organomet. Chem.* **1991**, *32*, 325.

(2) Xie, Z. *Acc. Chem. Res.* **2003**, *36*, 1.

(3) (a) Xie, Z.; Chui, K.; Yang, Q.; Mak, T. C. W. *Organometallics* **1999**, *18*, 3947. (b) Chui, K.; Yang, Q.; Mak, T. C. W.; Xie, Z. *Organometallics* **2000**, *19*, 1391. (c) Hong, E.; Kim, Y.; Do, Y. *Organometallics* **1998**, *17*, 2933.

(4) (a) Xie, Z.; Wang, S.; Zhou, Z.-Y.; Xue, F.; Mak, T. C. W. *Organometallics* **1998**, *17*, 489. (b) Xie, Z.; Wang, S.; Zhou, Z.-Y.; Mak, T. C. W. *Organometallics* **1998**, *17*, 1907. (c) Xie, Z.; Wang, S.; Zhou, Z.-Y.; Mak, T. C. W. *Organometallics* **1999**, *18*, 1641.

(5) (a) Zi, G.; Yang, Q.; Mak, T. C. W.; Xie, Z. *Organometallics* **2001**, *20*, 2359. (b) Lee, M.-H.; Hwang, J.-W.; Kim, Y.; Do, Y. *Organometallics* **2000**, *19*, 5514.

(6) Wang, S.; Yang, Q.; Mak, T. C. W.; Xie, Z. *Organometallics* **2000**, *19*, 334.

(7) (a) Xie, Z.; Wang, S.; Yang, Q.; Mak, T. C. W. *Organometallics* **1999**, *18*, 2420. (b) Wang, S.; Yang, Q.; Mak, T. C. W.; Xie, Z. *Organometallics* **1999**, *18*, 4478. (c) Xie, Z.; Wang, S.; Yang, Q.; Mak, T. C. W. *Organometallics* **1999**, *18*, 1578. (d) Wang, S.; Yang, Q.; Mak, T. C. W.; Xie, Z. *Organometallics* **1999**, *18*, 5511.

(8) Wang, S.; Li, H.-W.; Xie, Z. *Organometallics* **2001**, *20*, 3624.

(9) Wang, S.; Li, H.-W.; Xie, Z. *Organometallics* **2001**, *20*, 3842.

(10) Zi, G.; Li, H.-W.; Xie, Z. *Organometallics* **2002**, *21*, 1136.

(11) Wang, H.; Wang, Y.; Li, H.-W.; Xie, Z. *Organometallics* **2001**, *20*, 5110.

(12) Zi, G.; Li, H.-W.; Xie, Z. *Organometallics* **2002**, *21*, 3850.

10.1021/om034268l CCC: $27.50
Publication on Web 01/20/2004

other hand, they have very different electronic characteristics. According to the formal oxidation state of the phosphorus, two classes of complexes have been studied: (1) metallocenes bridged by four-coordinate phosphorus moieties where formal pentavalent phosphorus bears one positive charge[14] and (2) metallocenes bridged with three-coordinate phosphorus linkages, where trivalent phosphorus possesses one lone pair of electrons.[15] Phosphorus-bridged ansa ligands have demonstrated an interesting and rich chemistry.[14−16] In this regard, we have incorporated the R_2NP linkage into our carboranyl−indenyl hybrid ligand systems. It is hoped that a series of closely related complexes, $[A(C_9H_6)(C_2B_{10}H_{10})]MX_n$, which differ in the nature of the ansa bridge, will allow the features responsible for the various ansa effects (linkage effects) to be ascertained. We report here the design and synthesis of a new phosphorus-bridged hybrid ligand, $^i Pr_2NP(C_9H_7)(C_2B_{10}H_{11})$, and its applications in rare-earth chemistry.

Experimental Section

General Procedures. All experiments were performed under an atmosphere of dry dinitrogen, with the rigid exclusion of air and moisture using standard Schlenk or cannula techniques, or in a glovebox. All organic solvents were freshly distilled from sodium benzophenone ketyl immediately prior to use. $^i Pr_2NPCl_2$,[17] $Li_2C_2B_{10}H_{10}$,[4] KCH_2Ph,[18] and $Ln[N(SiHMe_2)_2]_3(THF)_2$[19] were prepared according to literature methods. All other chemicals were purchased either from Aldrich or Acros Chemical Co. and used as received unless otherwise noted. Infrared spectra were obtained from KBr pellets prepared in the glovebox on a Perkin-Elmer 1600 Fourier transform spectrometer. ^1H and ^{13}C NMR spectra were recorded on a Bruker DPX 300 spectrometer at 300.13 and 75.47 MHz, respectively. ^{11}B and ^{31}P NMR spectra were recorded on a Varian Inova 400 spectrometer at 128.32 and 161.91 MHz, respectively. All chemical shifts are reported in δ units with reference to the residual protons of the deuterated solvents for proton and carbon chemical shifts, to external $BF_3{\cdot}OEt_2$ (0.00 ppm) for boron chemical shifts, and to external 85% H_3PO_4 (0.00 ppm) for phosphorus chemical shifts. Elemental analyses were performed by MEDAC Ltd., Brunel University, Middlesex, U.K.

Preparation of $^i Pr_2NP(C_9H_7)Cl$ (1). A 1.6 M solution of *n*-BuLi in *n*-hexane (31.5 mL, 50.4 mmol) was added dropwise to a diethyl ether solution (250 mL) of indene (5.758 g, 50.0 mmol) at −78 °C, and the mixture was stirred for 6 h at room temperature. The precipitate (C_9H_7Li) was filtered off, washed with *n*-hexane (50 mL × 2), and dried under vacuum. This white solid was added in one portion to an *n*-hexane (300 mL) solution of $^i Pr_2NPCl_2$ (15.154 g, 75.0 mmol) at −78 °C with stirring. The reaction mixture was then stirred overnight at room temperature. After filtration, the solvent and excess $^i Pr_2NPCl_2$ were removed under vacuum, giving a yellow solid. Recrystallization from *n*-hexane afforded **1** as colorless crystals (8.735 g, 62%). ^1H NMR (benzene-d_6): δ 7.66 (d, J = 7.5 Hz, 1H, indenyl), 7.24 (m, 1H, indenyl), 7.21 (m, 1H, indenyl), 7.16 (m, 1H, indenyl), 7.11 (m, 1H, indenyl), 3.76 (br s, 2H, NC*H*$(CH_3)_2$), 3.05 (m, 2H, indenyl), 1.31 (br s, 6H, NCH(C*H*$_3)_2$), 1.09 (br s, 3H, NCH(C*H*$_3)_2$), 0.61 (br s, 3H, NCH(C*H*$_3)_2$). ^{13}C NMR (benzene-d_6): δ 145.2 (d, $^3J_{PC}$ = 7.4 Hz), 144.5 (d, $^2J_{PC}$ = 10.4 Hz), 144.3 (d, $^2J_{PC}$ = 22.3 Hz), 142.7 (d, $^1J_{PC}$ = 29.3 Hz), 126.3, 125.5, 124.3, 121.3, 39.5 (d, $^3J_{PC}$ = 1.4 Hz), (*C*$_9$H$_7$), 52.1 (br), 46.1 (br) (N*C*HMe$_2$), 31.9, 23.0, 19.7, 14.3 (NCH(*C*H$_3)_2$). ^{31}P NMR (benzene-d_6): δ 120.2. IR (KBr, cm^{-1}): ν 3063 (m), 2968 (vs), 2717 (m), 1456 (s), 1386 (s), 1263 (s), 1018 (vs), 916 (m) 875 (vs), 758 (vs), 717 (m), 633 (m). Anal. Calcd for $C_{15}H_{21}ClNP$: C, 63.94; H, 7.51; N, 4.97. Found: C, 63.61; H, 7.32; N, 5.00.

Preparation of $[^i Pr_2NP(C_9H_6)(C_2B_{10}H_{10})]Li_2(OEt_2)_{1.5}$ (2). A 1.6 M solution of *n*-BuLi in *n*-hexane (13.0 mL, 20.8 mmol) was slowly added to a stirred solution of *o*-$C_2B_{10}H_{12}$ (1.500 g, 10.4 mmol) in toluene/diethyl ether (2:1, 30 mL) at 0 °C, and the mixture was stirred at room temperature for 3 h. The resulting $Li_2C_2B_{10}H_{10}$ solution was then cooled to 0 °C, to which was slowly added a solution of $^i Pr_2NP(C_9H_7)Cl$ (2.930 g, 10.4 mmol) in toluene/diethyl ether (2:1, 30 mL). The reaction mixture was then stirred overnight. The white precipitate (LiCl) was filtered off. A 1.6 M solution of *n*-BuLi in *n*-hexane (6.5 mL, 10.4 mmol) was added dropwise to the resulting solution with stirring at −78 °C. This mixture was then stirred at room temperature overnight. After filtration, the solvent was concentrated to about 10 mL. **2** was isolated as a white crystalline solid (3.727 g, 70%) after this solution stood at −30 °C overnight. ^1H NMR (pyridine-d_5): δ 8.59 (d, J = 7.8 Hz, 1H, indenyl), 7.95 (d, J = 3.6 Hz, 1H, indenyl), 7.87 (d, J = 7.8 Hz, 1H, indenyl), 7.11 (t, J = 7.8 Hz, 1H, indenyl), 7.02 (t, J = 7.8 Hz, 1H, indenyl), 6.83 (d, J = 3.6 Hz, 1H, indenyl), 4.96 (br s, 2H) (NC*H*$(CH_3)_2$), 3.35 (q, J = 7.0 Hz, 6H, O(C*H*$_2$-CH$_3)_2$), 1.60 (br s, 3H, NCH(C*H*$_3)_2$), 1.55 (br s, 3H, NCH(C*H*$_3)_2$), 1.37 (br s, 3H, NCH(C*H*$_3)_2$), 1.12 (t, J = 7.0 Hz, 9H, O(CH$_2$C*H*$_3)_2$), 0.72 (br s, 3H, NCH(C*H*$_3)_2$). ^{13}C NMR (pyridine-d_5): δ 137.8 (d, $^2J_{PC}$ = 51.0 Hz), 131.7 (d, $^3J_{PC}$ = 11.1 Hz), 127.5 (d, $^1J_{PC}$ = 52.1 Hz), 120.1, 118.9, 118.8, 114.6, 113.7, 101.31 (*C*$_9$H$_6$), 93.9, 86.1 (d, $^1J_{PC}$ = 76.8 Hz) (cage *C*), 65.2, 14.9 (Et$_2$O), 49.0, 48.4 (N*C*HMe$_2$), 30.9, 25.6, 21.8, 15.1 (NCH(*C*H$_3)_2$). ^{11}B NMR (pyridine-d_5): δ −3.4 (5B), −6.4 (2B), −8.8 (3B). ^{31}P NMR (pyridine-d_5): δ 40.8. IR (KBr, cm^{-1}): ν 3107 (w), 2973 (vs), 2883 (s), 2562 (s), 1455 (s), 1366 (s), 1259 (s), 1170 (s), 1041 (s), 964 (s), 754 (s). Anal. Calcd for $C_{23}H_{45}B_{10}Li_2NO_{1.5}P$: C, 53.89; H, 8.85; N, 2.73. Found: C, 53.94; H, 8.86; N, 2.94.

Preparation of $^i Pr_2NP(C_9H_7)(C_2B_{10}H_{11})$ (4). A CH_2Cl_2 (40 mL) solution of Me_3NHCl (240 mg, 2.5 mmol) was added to a CH_2Cl_2 (20 mL) solution of $[^i Pr_2NP(C_9H_6)(C_2B_{10}H_{10})]Li_2(OEt_2)_{1.5}$ (**2**; 512 mg, 1.0 mmol) with stirring at 0 °C. This reaction

(13) Pauling, L. *The Nature of The Chemical Bond*, 3rd ed.; Cornell University Press: Ithaca, NY, 1960; p 224.

(14) (a) Shin, J. H.; Bridgewater, B. M.; Parkin, G. *Organometallics* **2000**, *19*, 5155. (b) Brady, E. D.; Hanusa, T. P.; Pink, M.; Young, V. G. *Inorg. Chem*. **2000**, *39*, 6028. (c) Leyser, N.; Schmidt, K.; Brintzinger, H.-H. *Organometallics* **1998**, *17*, 2155. (d) Taillefer, M.; Inguimbert, N.; Jäger, L.; Merzweiler, K.; Cristau, H.-J. *Chem. Commun*. **1999**, 565. (e) Harder, S.; Lutz, M. *Organometallics* **1997**, *16*, 225. (f) Peckham, T. J.; Lough, A. J.; Manners, I. *Organometallics* **1999**, *18*, 1030. (g) Shin, J. H.; Hascall, T.; Parkin, G. *Organometallics* **1999**, *18*, 6. (h) Schaverien, C. J.; Ernst, R.; Terlouw, W.; Schut, P.; Sudmerijer, O.; Budzelaar, P. H. M. *J. Mol. Catal. A: Chem*. **1998**, *128*, 245.

(15) (a) Malefetse, T. J.; Swiegers, G. F.; Coville, N. J.; Fernandes, M. A. *Organometallics* **2002**, *21*, 2898. (b) Kotov, V. V.; Avtomonov, E. V.; Sundermeyer, J.; Harms, K.; Lemenovskii, D. A. *Eur. J. Inorg. Chem*. **2002**, 678. (c) Ebels, J.; Pietschnig, R.; Kotila, S.; Dombrowski, A.; Niecke, E.; Nieger, M.; Schiffner, H. M. *Eur. J. Inorg. Chem*. **1998**, 331. (d) Alt, H. G.; Jung, M. *J. Organomet. Chem*. **1998**, *568*, 127. (e) Butchard, J. R.; Curnow, O. J.; Smail, S. J. *J. Organomet. Chem*. **1997**, *541*, 407. (f) Curnow, O. J.; Huttner, G.; Smail, S. J.; Turnbull, M. M. *J. Organomet. Chem*. **1996**, *524*, 267. (g) Fallis, K. A.; Anderson, G. K.; Rath, N. P. *Organometallics* **1992**, *11*, 885. (h) Anderson, G. K.; Lin, M. *Organometallics* **1988**, *7*, 2285. (i) Anderson, G. K.; Lin, M. *Inorg. Chim. Acta* **1988**, *142*, 7.

(16) (a) Mizuta, T.; Onishi, M.; Miyoshi, K. *Organometallics* **2000**, *19*, 5005. (b) Honeyman, C. H.; Peckham, T. J.; Massey, J. A.; Manners, I. *J. Chem. Soc., Chem. Commun*. **1996**, 2589. (c) Mizuta, T.; Yamasaki, T.; Nakazawa, H.; Miyoshi, K. *Organometallics* **1996**, *15*, 1093. (d) Honeyman, C. H.; Foucher, D. A.; Dahmen, F. Y.; Rulkens, R.; Lough, A. J.; Manner, I. *Organometallics* **1995**, *14*, 5503. (e) Seyferth, D.; Withers, H. P. *Organometallics* **1982**, *1*, 1275. (f) Withers, H. P.; Seyferth, D.; Fellmann, J. D.; Garrou, P. E.; Martin, S. *Organometallics* **1982**, *1*, 1283.

(17) King, R. B.; Sadanani, N. D. *Synth. React. Inorg. Met.-Org. Chem*. **1985**, *15*, 149.

(18) Manfred, S.; Juergen. H. *Angew. Chem., Int. Ed. Engl*. **1973**, *12*, 508.

(19) Anwander, R.; Runte, O.; Eppinger, J.; Gerstberger, G.; Herdtweck, E.; Spiegler, M. *J. Chem. Soc., Dalton Trans*. **1998**, 847.

mixture was warmed to room temperature and stirred overnight. Removal of the solvent afforded a white solid that was extracted with hot *n*-hexane (30 mL × 3). Removal of *n*-hexane generated a white solid. Recrystallization from *n*-hexane gave **4**, a mixture of allylic and vinylic isomers, as colorless crystals (319 mg, 82%). ^{1}H NMR (benzene-d_6): δ 7.73−6.52 (m, 6H, indenyl), 3.65 (s, 1H, cage C*H*), 3.19 (br s, 1H, indenyl), 3.16 (m, 2H, NC*H*Me$_2$), 2.94 (s, 2H, indenyl), 1.05 (d, J = 6.3 Hz, 6H, NCH(CH_3)$_2$), 0.29 (d, J = 6.3 Hz, 3H, NCH(CH_3)$_2$), 0.12 (d, J = 6.3 Hz, 3H, NCH(CH_3)$_2$). ^{13}C NMR (benzene-d_6): δ 146.5 (d, $^1J_{PC}$ = 54.8 Hz), 144.5 (d, $^3J_{PC}$ = 5.7 Hz), 144.2 (br), 142.8 (d, $^3J_{PC}$ = 10.0 Hz), 142.4 (d, $^2J_{PC}$ = 21.4 Hz), 137.8 (br), 134.2, 131.7, 127.3 (br), 126.7, 125.7, 124.8 (d, $^3J_{PC}$ = 5.1 Hz), 124.7, 124.3, 121.4, 121.1 (d, $^2J_{PC}$ = 19.0 Hz), 53.4 (d, $^1J_{PC}$ = 55.4 Hz), 40.5 (*C*$_9$H$_7$), 77.8 (d, $^2J_{PC}$ = 15.5 Hz), 76.8 (br), 65.6 (d, $^1J_{PC}$ = 42.0 Hz), 64.8 (d, $^1J_{PC}$ = 59.0 Hz) (cage *C*), 53.1 (d, $^2J_{PC}$ = 35.0 Hz), 51.9 (br), 44.9 (br), 44.8 (d, $^2J_{PC}$ = 45 Hz) (N*C*HMe$_2$), 31.9, 24.0, 21.4, 15.6 (NCH(*C*H$_3$)$_2$). ^{11}B NMR (benzene-d_6): δ −1.6 (3B), −7.3 (1B), −7.9 (1B), −10.4 (2B), −11.9 (1B), −13.1 (2B). ^{31}P NMR (benzene-d_6): δ 74.1, 40.1 (br) with an intensity ratio of 0.7:1. IR (KBr, cm^{-1}): ν 3069 (w), 2966 (m), 2888 (w), 2583 (s), 1599 (m), 1453 (m), 1371 (m), 1262 (w), 1165 (m), 1117 (m), 1019 (m), 794 (s), 720 (s). Anal. Calcd for $C_{17}H_{32}B_{10}NP$: C, 52.42; H, 8.28; N, 3.60. Found: C, 52.39; H, 8.26; N, 3.56.

Preparation of [^{i}Pr$_2$NP(C$_9$H$_6$)(C$_2$B$_{10}$H$_{11}$)][Li(DME)$_3$] (3). A THF (20 mL) solution of **4** (390 mg, 1.0 mmol) was slowly added to a THF (20 mL) solution of **2** (512 mg, 1.0 mmol) with stirring at −78 °C. This mixture was warmed to room temperature and stirred overnight. The solvent was evaporated under vacuum to dryness, and the residue was extracted with Et_2O (10 mL × 2). The extractions were combined and evaporated under vacuum to give a crude product. Recrystallization from a mixed solvent of DME/*n*-hexane (5:1, 10 mL) afforded **3** as light blue crystals (399 mg, 60%). ^{1}H NMR (pyridine-d_5): δ 8.55 (d, J = 7.5 Hz, 1H, indenyl), 7.92 (d, J = 8.4 Hz, 1H, indenyl), 7.63 (m, 1H, indenyl), 7.16 (t, J = 7.5 Hz, 1H, indenyl), 7.03 (t, J = 8.4 Hz, 2H, indenyl), 4.77 (br s, 2H, NC*H*Me$_2$), 4.11 (br s, 1H, cage C*H*), 3.49 (s, 12H, DME), 3.26 (s, 18H, DME), 1.44 (br s, 6H, NCH(CH_3)$_2$), 1.34 (br s, 3H, NCH(CH_3)$_2$), 0.95 (br s, 3H, NCH(CH_3)$_2$). ^{13}C NMR (pyridine-d_5): δ 138.7 (d, $^2J_{PC}$ = 53.0 Hz), 132.6 (d, $^3J_{PC}$ = 13.2 Hz), 128.4 (d, $^1J_{PC}$ = 74.0 Hz), 121.8, 118.7 (d, $^3J_{PC}$ = 2.8 Hz), 117.4 (d, $^2J_{PC}$ = 18.8 Hz), 114.5, 113.5, 102.7 (*C*$_9$H$_6$), 90.5, 84.1 (d, $^1J_{PC}$ = 99.8 Hz) (cage *C*), 71.4, 57.9 (DME), 50.7 (br), 44.4 (br) (N*C*HMe$_2$), 31.1, 22.2, 14.9, 13.6 (NCH(*C*H$_3$)$_2$). ^{11}B NMR (pyridine-d_5): δ −4.0 (2B), −7.9 (3B), −12.1 (5B). ^{31}P NMR (pyridine-d_5): δ 46.1. IR (KBr, cm^{-1}): ν 3070 (w), 2966 (s), 2834 (s), 2590 (vs), 1582 (w), 1459 (m), 1397 (m), 1365 (s), 1198 (s), 1082 (vs), 866 (s), 734 (s). Anal. Calcd for $C_{29}H_{61}B_{10}LiNO_6P$: C, 52.31; H, 9.23; N, 2.10. Found: C, 52.43; H, 8.93; N, 2.46.

Preparation of [η^5:σ-^{i}Pr$_2$NP(C$_9$H$_6$)(C$_2$B$_{10}$H$_{10}$)]Yb(DME)$_2$ (5). A THF (15 mL) solution of **2** (256 mg, 0.5 mmol) was added dropwise to a THF (15 mL) solution of $YbI_2(THF)_x$ (10.4 mL, 0.5 mmol) at 0 °C, and the reaction mixture was stirred at room temperature overnight. After removal of THF, the residue was extracted with a mixed solvent of toluene and DME (5:1, 15 mL × 2). The resulting solutions were combined and concentrated to about 15 mL. **5** was isolated as orange-red crystals after this solution stood at room temperature for 6 days (259 mg, 70%). ^{1}H NMR (pyridine-d_5): δ 8.21 (d, J = 8.1 Hz, 1H, indenyl), 7.92 (s, 1H, indenyl), 7.11 (d, J = 8.1 Hz, 1H, indenyl), 7.01 (t, J = 6.9 Hz, 1H, indenyl), 6.82 (t, J = 6.9 Hz, 1H, indenyl), 6.70 (s, 1H, indenyl), 4.69 (br s, 2H, NC*H*Me$_2$), 3.48 (s, 8H, DME), 3.26 (s, 12H, DME), 1.47 (d, J = 7.2 Hz, 6H, NCH(CH_3)$_2$), 1.17 (br s, 3H, NCH(CH_3)$_2$), 0.70 (br s, 3H, NCH(CH_3)$_2$).^{13}C NMR (pyridine-d_5): δ 128.2 (d, $^2J_{PC}$ = 10.0 Hz), 122.1, 120.8, 120.4 (d, $^1J_{PC}$ = 19.0 Hz), 118.3, 117.5, 111.6, 101.8 (d, $^2J_{PC}$ = 10.3 Hz), 101.2 (*C*$_9$H$_6$), 89.1, 87.9 (d, $^1J_{PC}$ = 61.9 Hz) (cage *C*), 71.4, 57.9 (DME), 50.6 (d, $^2J_{PC}$ = 14.3 Hz), 44.1 (d, $^2J_{PC}$ = 35.8 Hz) (N*C*HMe$_2$), 31.0, 25.3, 21.7 (d, $^3J_{PC}$ = 20.3 Hz), 13.6 (NCH(*C*H$_3$)$_2$). ^{11}B NMR (pyridine-d_5): δ −3.0 (4B), −7.6 (6B). ^{31}P NMR (pyridine-d_5): δ 35.5. IR (KBr, cm^{-1}): ν 3056 (w), 2961 (s), 2932 (s), 2596 (vs), 1637 (w), 1456 (m), 1362 (m), 1329 (s), 1195 (s), 1063 (vs), 861 (s), 755 (s). Anal. Calcd for $C_{21}H_{40}B_{10}NO_2PYb$ (**5**−DME): C, 38.76; H, 6.20; N, 2.15. Found: C, 38.61; H, 6.56; N, 1.89.

Preparation of [{η^5:σ-^{i}Pr$_2$NP(C$_9$H$_6$)(C$_2$B$_{10}$H$_{10}$)}$_2$Yb][Li(THF)$_3$(Et$_2$O)] (6). A THF (10 mL) solution of **3** (166 mg, 0.3 mmol) was added dropwise to a THF (10 mL) solution of **5** (185 mg, 0.3 mmol) with stirring at room temperature, and the mixture was stirred for 8 h. After removal of THF, the residue was extracted with Et_2O/THF (10:1, 10 mL × 4). The extractions were combined and concentrated to about 10 mL. **6** was isolated as green crystals after this solution stood at −30 °C for 5 days (93 mg, 30%). ^{1}H NMR (pyridine-d_5): many broad, unresolved resonances. ^{13}C NMR (pyridine-d_5): δ 66.9, 24.9 (THF), plus many broad, unresolved resonances. ^{11}B NMR (pyridine-d_5): δ −0.2 (1B), −1.4 (5B), −4.3 (2B), −5.8 (2B). ^{31}P NMR (pyridine-d_5): δ 42.9. IR (KBr, cm^{-1}): ν 3040 (w), 2966 (s), 2574 (vs), 1453 (m), 1386 (m), 1360 (m), 1159 (m), 1072 (vs), 1040 (s), 874 (m), 798 (m), 742 (m). Anal. Calcd for $C_{34}H_{60}B_{20}LiN_2P_2Yb$ (**6**−3THF·Et$_2$O): C, 42.76; H, 6.33; N, 2.93. Found: C, 42.58; H, 6.76; N, 2.60.

This complex was also obtained in 59% yield from the reaction of $YbCl_3$ with **2** in THF in a molar ratio of 1:2.

Preparation of [{η^5:σ-^{i}Pr$_2$NP(C$_9$H$_6$)(C$_2$B$_{10}$H$_{10}$)}$_2$Sm][Li(DME)$_3$] (7). A THF (15 mL) solution of **2** (512 mg, 1.0 mmol) was added dropwise to a THF solution of $SmI_2(THF)_x$ (18.5 mL, 1.0 mmol), and the reaction mixture was stirred overnight at room temperature. The color of the solution changed from dark blue to dark red during the course of the reaction. The solvent was evaporated under vacuum, leaving an oily residue that was washed with hot toluene (10 mL × 2). The resulting solid was extracted with a mixed solvent of toluene and DME (2:1, 10 mL × 2). The solutions were combined and concentrated to about 10 mL, from which **7** was obtained as orange crystals after this solution stood at room temperature for 4 days (433 mg, 36%). ^{1}H NMR (pyridine-d_5): 3.50 (s), 3.27 (s) (DME), plus many broad, unresolved peaks. ^{13}C NMR (pyridine-d_5): δ 71.4, 58.0 (DME), plus many broad, unresolved peaks. ^{11}B NMR (pyridine-d_5): δ −3.4 (3B), −5.9 (5B), −9.8 (1B), −13.9 (1B). ^{31}P NMR (pyridine-d_5): δ 47.1, 44.6 (equal intensity). IR (KBr, cm^{-1}): ν 2964 (s), 2926 (s), 2570 (vs), 1455 (m), 1369 (m), 1259 (m), 1161 (m), 1080 (vs), 962 (m), 866 (w), 797 (m), 737 (w). Anal. Calcd for $C_{46}H_{90}B_{20}LiN_2O_6P_2Sm$: C, 45.94; H, 7.54; N, 2.33. Found: C, 46.57; H, 7.58; N, 2.10.

This complex was also obtained in 45% yield from the reaction of $SmCl_3$ with **2** in a molar ratio of 1:2.

Preparation of [{η^5:σ-^{i}Pr$_2$NP(C$_9$H$_6$)(C$_2$B$_{10}$H$_{10}$)}$_2$Nd][Li(DME)$_3$] (8). A THF (10 mL) solution of **2** (512 mg, 1.0 mmol) was slowly added to a suspension of $NdCl_3$ (125 mg, 0.5 mmol) in THF (15 mL) with stirring at room temperature, followed by the identical procedure reported for **7** to give **8** as dark blue crystals (251 mg, 42%). ^{1}H NMR (pyridine-d_5): δ 3.48 (s), 3.25 (s) (DME), plus many broad, unresolved peaks. ^{13}C NMR (pyridine-d_5): 72.4, 58.9 (DME), plus many broad, unresolved peaks. ^{11}B NMR (pyridine-d_5): many broad, unresolved resonances. ^{31}P NMR (pyridine-d_5): δ 44.1, 32.5 (equal intensity). IR (KBr, cm^{-1}): ν 2964 (s), 2577 (vs), 1456 (w), 1375 (w), 1259 (m), 1081 (vs), 1025 (s), 800 (s), 530 (m). Anal. Calcd for $C_{46}H_{90}B_{20}LiN_2NdO_6P_2$: C, 46.17; H, 7.58; N, 2.34. Found: C, 46.49; H, 7.54; N, 2.56.

Preparation of [{η^5:σ-^{i}Pr$_2$NP(C$_9$H$_6$)(C$_2$B$_{10}$H$_{10}$)}$_2$Er][Li(DME)$_3$] (9). This complex was prepared as a pink crystalline solid from reaction of $ErCl_3$ (137 mg, 0.5 mmol) with **2** (512 mg, 1.0 mmol) in THF (15 mL) using the same procedure reported for **7**: yield 310 mg (51%). ^{1}H NMR (pyridine-d_5): δ 3.50 (s), 3.27 (s) (DME), plus many broad, unresolved peaks. ^{13}C NMR (pyridine-d_5): δ 72.0, 58.5 (DME), plus many broad, unresolved peaks. ^{11}B NMR (pyridine-d_5): δ −5.3 (2B), −10.1 (1B), −11.8 (2B), −15.8 (4B), −16.7 (1B). ^{31}P NMR (pyridine-

d_5): δ 45.9. IR (KBr, cm^{-1}): ν 2960 (s), 2915 (s), 2572 (s), 1457 (m), 1378 (m), 1259 (s), 1088 (s), 1019 (s), 801 (s), 536 (s). Anal. Calcd for $C_{46}H_{90}B_{20}ErLiN_2O_6P_2$: C, 45.30; H, 7.44; N, 2.30. Found: C, 45.76; H, 7.47; N, 2.49.

Preparation of [{η^5:σ-^{i}Pr$_2$NP(C$_9$H$_6$)(C$_2$B$_{10}$H$_{10}$)}$_2$Y][Li(DME)$_2$(THF)] (10). This complex was prepared as colorless crystals from reaction of YCl_3 (97 mg, 0.5 mmol) with **2** (512 mg, 1.0 mmol) in THF (30 mL) using the identical procedure reported for **7**: yield 387 mg (69%). ^{1}H NMR (pyridine-d_5): δ 7.78 (d, J = 6.0 Hz, 2H, indenyl), 7.39 (br s, 2H, indenyl), 7.14 (dd, J = 6.9 and 7.5 Hz, 2H, indenyl), 6.95 (dd, J = 7.5 and 6.9 Hz, 2H, indenyl), 6.81 (d, J = 8.4 Hz, 2H, indenyl), 6.64 (d, J = 3.3 Hz, 2H, indenyl), 4.38 (br s, 4H, NC*H*Me$_2$), 3.69 (m, 4H, THF), 3.48 (s, 8H, DME), 3.25 (s, 12H, DME), 1.60 (m, 4H, THF), 1.32 (d, J = 6.3 Hz, 6H, NCH(C*H*$_3$)$_2$), 1.23 (d, J = 6.0 Hz, 6H, NCH(C*H*$_3$)$_2$), 0.93 (d, J = 6.3 Hz, 6H, NCH(C*H*$_3$)$_2$), 0.53 (d, J = 6.0 Hz, 6H, NCH(C*H*$_3$)$_2$). ^{13}C NMR (pyridine-d_5): δ 132.2 (d, $^1J_{PC}$ = 45.3 Hz), 128.7, 127.9, 124.9 (d, $^3J_{PC}$ = 9.1 Hz), 122.3, 120.7, 119.6 (d, $^3J_{PC}$ = 20.9 Hz), 110.8 (d, $^3J_{PC}$ = 15.4 Hz), 108.5 (*C*$_9$H$_6$), 89.9 (d, $^1J_{PC}$ = 60.7 Hz), 80.3 (cage *C*), 71.3, 57.9 (DME), 66.3, 24.2 (THF), 50.64 (d, $^2J_{PC}$ = 11.1 Hz), 44.25 (d, $^2J_{PC}$ = 35.6 Hz) (N*C*HMe$_2$), 31.0, 25.1 (d, $^3J_{PC}$ = 9.8 Hz), 24.76 (d, $^3J_{PC}$ = 21.0 Hz), 22.2 (NCH(*C*H$_3$)$_2$). ^{11}B NMR (pyridine-d_5): δ −3.1 (6B), −8.6 (4B). ^{31}P NMR (pyridine-d_5): δ 33.0. IR (KBr, cm^{-1}): ν 3059 (w), 2965 (s), 2578 (vs), 2548 (vs), 1454 (s), 1388 (m), 1258 (m), 1119 (s), 1077 (vs), 868 (m), 780 (m). Anal. Calcd for $C_{46}H_{88}B_{20}LiN_2O_5P_2Y$: C, 49.19; H, 7.90; N, 2.49. Found: C, 48.93; H, 7.81; N, 2.60.

This complex was also obtained in 35% yield from the reaction of [{[η^5:σ-^{i}Pr$_2$NP(C$_9$H$_6$)(C$_2$B$_{10}$H$_{10}$)]YCl}$_2$(μ-Cl)$_3$Li(DME)]-[Li(DME)$_3$]$_2$ (**12**) with LiN(SiMe$_3$)$_2$ in a molar ratio of 1:2.

Preparation of [{[η^5:σ-^{i}Pr$_2$NP(C$_9$H$_6$)(C$_2$B$_{10}$H$_{10}$)]ErCl}$_2$(μ-Cl)$_3$Li(DME)][Li(DME)$_3$]$_2$ (11). A THF solution (15 mL) of **2** (512 mg, 1.0 mmol) was slowly added to a THF suspension (10 mL) of $ErCl_3$ (273 mg, 1.0 mmol) at −20 °C, and the mixture was then stirred at room temperature overnight. After removal of the precipitate and the solvent, the residue was extracted with hot toluene (10 mL × 2) and a mixed solvent of hexane and DME (3:1, 10 mL × 2), respectively. The solutions were combined and concentrated to about 10 mL. **11** was obtained as pink crystals after this solution stood at room temperature for 6 days (891 mg, 46%). ^{1}H NMR (pyridine-d_5): δ 3.46 (s), 3.23 (s) (DME), plus many broad, unresolved peaks. ^{13}C NMR (pyridine-d_5): many broad, unresolved peaks. ^{11}B NMR (pyridine-d_5): δ −6.3 (1B), −7.8 (2B), −11.5 (2B), −12.7 (2B), −15.9 (1B), −16.8 (1B), −17.6 (1B). ^{31}P NMR (pyridine-d_5): δ 41.7. IR (KBr, cm^{-1}): ν 2962 (s), 2929 (s), 2591 (vs), 1454 (m), 1259 (m), 1082 (vs), 1024 (s), 797 (m), 527 (m). Anal. Calcd for $C_{62}H_{130}B_{20}Cl_5Er_2Li_3N_2O_{14}P_2$: C, 38.42; H, 6.76; N, 1.45. Found: C, 38.30; H, 6.31; N, 1.79.

Preparation of [{[η^5:σ-^{i}Pr$_2$NP(C$_9$H$_6$)(C$_2$B$_{10}$H$_{10}$)]YCl}$_2$(μ-Cl)$_3$Li(DME)][Li(DME)$_3$]$_2$ (12). This complex was obtained as pale yellow crystals from the reaction of **2** (512 mg, 1.0 mmol) with YCl_3 (195 mg, 1.0 mmol) in THF (30 mL) using the identical procedure reported for **11**: yield 908 mg (51%). ^{1}H NMR (pyridine-d_5): δ 7.77 (d, J = 8.3 Hz, 2H, indenyl), 7.38 (br s, 2H, indenyl), 7.13 (t, J = 8.3 Hz, 2H, indenyl), 6.96 (t, J = 8.3 Hz, 2H, indenyl), 6.80 (d, J = 8.3 Hz, 2H, indenyl), 6.63 (d, J = 3.0 Hz, 2H, indenyl), 4.38 (m, 2H, NC*H*Me$_2$), 3.48 (s, 28H, DME), 3.25 (s, 42H, DME), 3.05 (m, 2H, NC*H*Me$_2$), 1.32 (d, J = 5.4 Hz, 6H, NCH(C*H*$_3$)$_2$), 1.22 (d, J = 6.3 Hz, 6H, NCH(C*H*$_3$)$_2$), 0.93 (d, J = 6.3 Hz, 6H, NCH(C*H*$_3$)$_2$), 0.53 (d, J = 6.0 Hz, 6H, NCH(C*H*$_3$)$_2$). ^{13}C NMR (pyridine-d_5): δ 136.0, 133.4 (d, $^3J_{PC}$ = 20.9 Hz), 129.4 (d, $^1J_{PC}$ = 74.4 Hz), 122.7 (d, $^2J_{PC}$ = 46.4 Hz), 119.4, 118.3 (d, $^3J_{PC}$ = 25.5 Hz), 115.2, 114.4 (d, $^2J_{PC}$ = 41.0 Hz), 103.4 (*C*$_9$H$_6$), 91.3 (d, $^2J_{PC}$ = 35.5 Hz), 84.5 (d, $^1J_{PC}$ = 55.6 Hz) (cage *C*), 72.1, 58.6 (DME), 51.3 (br), 45.0 (br) (N*C*HMe$_2$), 31.7, 29.2, 22.7 (d, $^3J_{PC}$ = 18.0 Hz), 13.6 (NCH(*C*H$_3$)$_2$).^{11}B NMR (pyridine-d_5): δ −0.3 (1B), −1.3 (2B), −5.2 (2B), −6.7 (1B), −9.5 (1B), −10.9 (2B), −11.7 (1B). ^{31}P NMR (pyridine-d_5): δ 45.6. IR (KBr, cm^{-1}): ν 2962 (s), 2584 (vs), 1632 (s), 1261 (s), 1093 (vs), 1026 (vs), 802 (s), 499 (m). Anal. Calcd for $C_{62}H_{130}B_{20}Cl_5Li_3N_2O_{14}P_2Y_2$: C, 41.79; H, 7.35; N, 1.57. Found: C, 41.77; H, 7.15; N, 1.74.

Preparation of {[η^5:σ-^{i}Pr$_2$NP(C$_9$H$_6$)(C$_2$B$_{10}$H$_{10}$)]$_2$Y}{(η^6-C$_6$H$_5$CH$_3$)$_2$K} (13). A THF solution (15 mL) of KCH_2Ph (150 mg, 1.0 mmol) was slowly added to a stirred THF solution (15 mL) of **12** (890 mg, 0.5 mmol) at −78 °C. The reaction mixture was warmed to room temperature and stirred overnight. After removal of the precipitate and the solvent under vacuum, the oily residue was extracted with toluene (10 mL × 2). The resulting toluene solutions were combined and concentrated to about 10 mL, to which was added 5 mL of *n*-hexane. **13** was obtained as pale yellow crystals after this solution stood at −20 °C for 6 days (309 mg, 57%). ^{1}H NMR (pyridine-d_5): δ 7.78 (d, J = 6.9 Hz, 2H, indenyl), 7.39 (br s, 2H, indenyl), 7.24 (m, 10H, C$_6$*H*$_5$CH$_3$), 7.13 (t, J = 6.9 Hz, 2H, indenyl), 6.95 (t, J = 6.9 Hz, 2H, indenyl), 6.80 (d, J = 6.9 Hz, 2H, indenyl), 6.64 (d, J = 3.0 Hz, 2H, indenyl), 4.38 (m, 2H, NC*H*Me$_2$), 3.06 (m, 2H, NC*H*Me$_2$), 2.20 (s, 6H, PhC*H*$_3$), 1.32 (d, J = 3.3 Hz, 6H, NCH(C*H*$_3$)$_2$), 1.22 (d, J = 6.0 Hz, 6H, NCH(C*H*$_3$)$_2$), 0.80 (d, J = 3.6 Hz, 6H, NCH(C*H*$_3$)$_2$), 0.53 (d, J = 6.0 Hz, 6H, NCH(C*H*$_3$)$_2$). ^{13}C NMR (pyridine-d_5): δ 127.9, 127.2, 124.2, 117.8 (d, $^3J_{PC}$ = 16.8 Hz), 116.5 (d, $^2J_{PC}$ = 33.0 Hz), 113.5 (d, $^1J_{PC}$ = 56.0 Hz), 112.7, 112.1, 101.8, 97.9 (*C*$_9$H$_6$ and *C*$_6$H$_5$CH$_3$), 95.5 (br), 82.4 (br) (cage *C*), 49.6 (br), 44.3 (br) (N*C*HMe$_2$), 30.2, 27.7, 21.3, 13.9 (NCH(*C*H$_3$)$_2$), 19.8 (C$_6$H$_5$C*H*$_3$). ^{11}B NMR (pyridine-d_5): δ −1.1 (6B), −6.8 (4B). ^{31}P NMR (pyridine-d_5): δ 41.2. IR (KBr, cm^{-1}): ν 3059 (w), 2960 (s), 2581 (vs), 1451 (w), 1381 (m), 1260 (s), 1086 (vs), 1030 (vs), 802 (s), 516 (m). Anal. Calcd for $C_{48}H_{76}B_{20}KN_2P_2Y$: C, 53.02; H, 7.05; N, 2.58. Found: C, 53.58; H, 6.99; N, 2.29.

Preparation of [{η^5:σ-^{i}Pr$_2$NP(C$_9$H$_6$)(C$_2$B$_{10}$H$_{10}$)}Y{(μ-H)$_3$BH}$_2$][Li(DME)$_3$] (14). A THF solution (10 mL) of **12** (890 mg, 0.5 mmol) was slowly added to a THF suspension (10 mL) of $NaBH_4$ (40 mg, 1.1 mmol), and the mixture was stirred at room temperature for 2 days. After removal of the white precipitate, the clear THF solution was concentrated under vacuum to about 10 mL, to which was added 5 mL of *n*-hexane. **14** was isolated as colorless crystals after this solution stood at −20 °C for 3 days (254 mg, 59%). ^{1}H NMR (pyridine-d_5): δ 8.65 (d, J = 7.8 Hz, 1H, indenyl), 7.69 (br s, 1H, indenyl), 7.31 (t, J = 7.8 Hz, 1H, indenyl), 7.26 (t, J = 7.8 Hz, 1H, indenyl), 7.02 (d, J = 3.6 Hz, 1H, indenyl), 6.98 (d, J = 3.6 Hz, 1H, indenyl), 4.67 (br s, 2H, NC*H*Me$_2$), 3.48 (s, 12H, DME), 3.26 (s, 18H, DME), 1.42 (d, J = 6.6 Hz, 9H, NCH(C*H*$_3$)$_2$), 1.09 (d, J = 6.9 Hz, 3H, NCH(C*H*$_3$)$_2$). ^{13}C NMR (pyridine-d_5): δ 129.4 (d, $^1J_{PC}$ = 72.8 Hz), 126.1, 119.7, 115.5, 114.5, 110.2, 107.4, 104.7 (d, $^2J_{PC}$ = 38.0 Hz), 103.7 (*C*$_9$H$_6$), 92.7 (br), 88.0 (d, $^1J_{PC}$ = 61.9 Hz) (cage *C*), 72.1, 58.6 (DME), 51.1 (br), 45.4 (br) (N*C*HMe$_2$), 32.1, 23.2, 21.7, 14.6 (NCH(*C*H$_3$)$_2$). ^{11}B NMR (pyridine-d_5): δ −1.5 (2B), −2.8 (1B), −4.2 (3B), −7.5 (4B), −30.8 (2B) (BH_4^- group). ^{31}P NMR (pyridine-d_5): δ 42.8. IR (KBr, cm^{-1}): ν 2953 (s), 2891 (s), 2577 (vs), 2393 (m), 2297 (m), 1675 (w), 1600 (s), 1458 (s), 1258 (m), 1123 (m), 1020 (s), 792 (s), 626 (m). Anal. Calcd for $C_{25}H_{58}B_{12}LiNO_4PY$ (**14**−DME): C, 43.31; H, 8.43; N, 2.02. Found: C, 43.57; H, 8.06; N, 1.82.

X-ray Structure Determination. All single crystals were immersed in Paratone-N oil and sealed under N_2 in thin-walled glass capillaries. Data were collected at 293 K on a Bruker SMART 1000 CCD diffractometer using Mo Kα radiation. An empirical absorption correction was applied using the SADABS program.[20] All structures were solved by direct methods and subsequent Fourier difference techniques and refined anisotropically for all non-hydrogen atoms by full-matrix least-squares calculations on F^2 using the SHELXTL program package.[21] Most of the carborane hydrogen atoms were located

(20) Sheldrick, G. M. SADABS: Program for Empirical Absorption Correction of Area Detector Data; University of Göttingen, Göttingen, Germany, 1996.

Table 1. Crystal Data and Summary of Data Collection and Refinement for 1 and 3−7

	1	3	4	5	6	7
formula	$C_{15}H_{21}ClNP$	$C_{29}H_{61}B_{10}LiNO_6P$	$C_{17}H_{32}B_{10}NP$	$C_{25}H_{50}B_{10}NO_4PYb$	$C_{50}H_{94}B_{20}LiN_2O_4P_2Yb$	$C_{46}H_{90}B_{20}LiN_2O_6P_2Sm$
cryst size (mm)	0.34 × 0.23 × 0.06	0.45 × 0.42 × 0.35	0.56 × 0.53 × 0.40	0.45 × 0.32 × 0.16	0.20 × 0.18 × 0.15	0.62 × 0.34 × 0.26
fw	281.8	665.8	389.5	740.8	1245.4	1202.6
cryst syst	monoclinic	triclinic	monoclinic	monoclinic	monoclinic	monoclinic
space group	$P2_1/n$	$P\bar{1}$	$P2_1/n$	$P2_1/c$	$P2_1/n$	$P2_1/n$
a, Å	13.364(4)	11.352(2)	10.215(1)	11.947(2)	24.441(5)	18.160(3)
b, Å	7.514(1)	13.204(3)	19.240(2)	18.032(4)	11.136(2)	18.178(3)
c, Å	15.789(5)	15.634(3)	11.858(2)	17.016(3)	26.313(5)	21.215(4)
α, deg	90	70.59(3)	90	90	90	90
β, deg	91.11(1)	69.87(3)	98.98(1)	102.45(3)	112.57(3)	102.99(1)
γ, deg	90	86.51(3)	90	90	90	90
V, Å^3	1585.3(7)	2071.4(7)	2302.1(4)	3579.5(12)	6613(2)	6824(2)
Z	4	2	4	4	4	4
D_{calcd}, Mg/m^3	1.180	1.067	1.124	1.375	1.251	1.171
radiation (*λ*), Å				Mo Kα (0.710 73)		
2*θ* range, deg	4.0−50.0	3.0−50.0	4.0−50.0	3.4−50.0	4.0−50.0	3.0−50.0
μ, mm^{-1}	0.326	0.103	0.124	2.687	1.503	0.948
F(000)	600	716	824	1496	2572	2492
no. of obsd rflns	2220	3902	4039	5480	5629	12 030
no. of params refnd	164	444	326	416	731	602
goodness of fit	1.131	1.118	0.933	1.073	0.982	1.063
R1	0.056	0.091	0.061	0.058	0.082	0.068
wR2	0.128	0.247	0.157	0.143	0.204	0.215

Table 2. Crystal Data and Summary of Data Collection and Refinement for 8 and 10−14

	8	10	11	12	13	14
formula	$C_{46}H_{90}B_{20}LiN_2NdO_6P_2$	$C_{46}H_{88}B_{20}LiN_2O_5P_2Y$	$C_{62}H_{130}B_{20}Cl_5Er_2Li_3N_2O_{14}P_2$	$C_{62}H_{130}B_{20}Cl_5Li_3N_2O_{14}P_2Y_2$	$C_{48}H_{76}B_{20}KN_2P_2Y$	$C_{29}H_{68}B_{12}LiNO_6PY$
cryst size (mm)	0.56 × 0.53 × 0.40	0.45 × 0.78 × 0.90	0.51 × 0.34 × 0.32	0.45 × 0.38 × 0.25	0.38 × 0.27 × 0.25	0.48 × 0.45 × 0.18
fw	1196.5	1123.2	1938.4	1781.7	1087.3	783.4
cryst syst	monoclinic	monoclinic	monoclinic	monoclinic	orthorhombic	monoclinic
space group	$P2_1/n$	$P2_1/c$	$P2_1/c$	$P2_1/c$	$P2_12_12_1$	$C2/c$
a, Å	18.167(3)	14.016(1)	21.605(1)	21.573(2)	13.610(2)	28.646(2)
b, Å	18.183(3)	13.643(1)	13.933(1)	13.936 (1)	20.136(2)	21.458(2)
c, Å	21.270(4)	33.688(2)	32.940(2)	32.960(3)	21.660(2)	20.066(1)
α, deg	90	90	90	90	90	90
β, deg	103.27(1)	99.64(1)	103.21(1)	103.19(1)	90	130.71(1)
γ, deg	90	90	90	90	90	90
V, Å^3	6839(2)	6350.8(6)	9653.0(8)	9647.8(12)	5936.0(10)	9349.7(9)
Z	4	4	4	4	4	8
D_{calcd}, Mg/m^3	1.162	1.175	1.334	1.227	1.217	1.113
radiation (*λ*), Å			Mo Kα (0.710 73)			
2*θ* range, deg	3.0−50.0	3.0−50.0	2.6−50.0	3.2−50.0	3.4−50.0	2.6−50.0
μ, mm^{-1}	0.847	1.010	1.949	1.419	1.142	1.316
F(000)	2484	2360	3952	3720	2264	3312
no. of obsd rflns	8946	9953	12 602	12 603	10 437	8243
no. of params refnd	703	693	833	832	646	493
goodness of fit	0.936	0.980	1.087	1.076	0.993	0.849
R1	0.080	0.039	0.073	0.093	0.058	0.056
wR2	0.210	0.103	0.192	0.251	0.121	0.132

from difference Fourier syntheses. All other hydrogen atoms were geometrically fixed using the riding model. Crystal data and details of data collection and structure refinements are given in Tables 1 and 2, respectively. Selected bond distances and angles are compiled in Tables 3 and 4, respectively. Further details are included in the Supporting Information.

Results and Discussion

Ligands. Our target phosphorus compound contains three different substituents that have to be introduced step by step. Reaction of PCl_3 with 2 equiv of $^iPr_2NH$ in *n*-hexane gave $^iPr_2NPCl_2$ in 78% yield.[17] Interaction between $^iPr_2NPCl_2$ and C_9H_7Li in a molar ratio of 1:1 in *n*-hexane afforded $^iPr_2NP(C_9H_7)Cl$ (**1**) in 62% yield. **1** reacted with 1 equiv of $Li_2C_2B_{10}H_{10}$ in toluene/ether (2:1) at −78 °C to give, after treatment with 1 equiv of *n*-BuLi, the dilithium salt $[^iPr_2NP(C_9H_6)(C_2B_{10}H_{10})]Li_2(OEt_2)_{1.5}$ (**2**) in 70% yield. Its neutral counterpart $^iPr_2NP(C_9H_7)(C_2B_{10}H_{11})$ cannot be prepared by hydrolysis, due to the presence of a moisture-sensitive P−C bond. An oxygen- and moisture-free procedure is thus desired. Treatment of **2** with 2.5 equiv of dry Me_3NHCl in CH_2Cl_2 gave, after extraction with hot *n*-hexane, the neutral compound $^iPr_2NP(C_9H_7)(C_2B_{10}H_{11})$ (**4**) in 82% yield. Mixing **2** and **4** in a 1:1 molar ratio in THF generated, after recrystallization from DME, the monolithium salt $[^iPr_2NP(C_9H_6)(C_2B_{10}H_{11})][Li(DME)_3]$ (**3**) in 60% yield. The above synthetic routes are summarized in Scheme 1.

(21) Sheldrick, G. M. SHELXTL 5.10 for Windows NT: Structure Determination Software Programs; Bruker Analytical X-ray Systems, Inc., Madison, WI, 1997.

Table 3. Selected Bond Lengths (Å) and Angles (deg) for 1 and 3−7[a]

	compd (Ln)					
	1	**3**	**4**	**5** (Yb)	**6** (Yb)	**7** (Sm)
P−N	1.652(2)	1.685(2)	1.673(2)	1.676(6)	1.664(15)	1.680(7)
P−C(cage)		1.929(2)	1.898(3)	1.872(7)	1.893(19)	1.891(9)
P−C(ring)	1.820(3)	1.768(2)	1.827(3)	1.799(6)	1.769(18)	1.801(8)
av Ln−C(ring)				2.790(8)	2.673(17)	2.752(8)
av Ln−C(cage)				2.587(7)	2.471(17)	2.578(8)
C(cage)−Ln−C(cage)					105.9(7)	106.3(3)
Cent−Ln−Cent					124.3	122.8
av C(cage)−P−C(ring)		101.7(1)	102.3(1)	109.4(3)	102.9(9)	101.2(3)
∑∠P	306.5(2)	316.2(1)	313.9(1)	317.8(3)	313.3(9)	315.9(4)
∑∠N	357.9(2)	358.4(2)	358.8(2)	359.1(6)	357.1(16)	358.8(8)

[a] Cent = the centroid of the five-membered ring of the indenyl group.

Table 4. Selected Bond Lengths (Å) and Angles (deg)[a] for 8 and 10−14

	compd (Ln)					
	8 (Nd)	**10** (Y)	**11** (Er)	**12** (Y)	**13** (Y)	**14** (Y)
P−N	1.703(6)	1.677(3)	1.671(12)	1.688(9)	1.678(3)	1.666(14)
P−C(cage)	1.887(7)	1.883(3)	1.878(12)	1.893(10)	1.884(3)	1.890(14)
P−C(ring)	1.796(7)	1.817(3)	1.844(11)	1.804(10)	1.811(3)	1.813(16)
av Ln−C(ring)	2.780(7)	2.703(3)	2.704(12)	2.719(10)	2.699(3)	2.663(18)
av Ln−C(cage)	2.612(7)	2.538(3)	2.526(12)	2.545(10)	2.544(3)	2.479(13)
C(cage)−Ln−C(cage)	108.4(2)	99.73(9)			98.36(10)	
Cent−Ln−Cent	122.8	136.1			137.0	
av C(cage)−P−C(ring)	101.1(3)	100.9(2)	100.2(5)	100.8(5)	101.3(1)	101.1(1)
∑∠P	316.1(4)	315.7(13)	314.4(5)	315.7(15)	316.0(14)	316.4(8)
∑∠N	358.0(6)	358.5(17)	357.5(13)	358.1(15)	358.0(3)	358.3(5)

[a] Cent = the centroid of the five-membered ring of the indenyl group.

Scheme 1

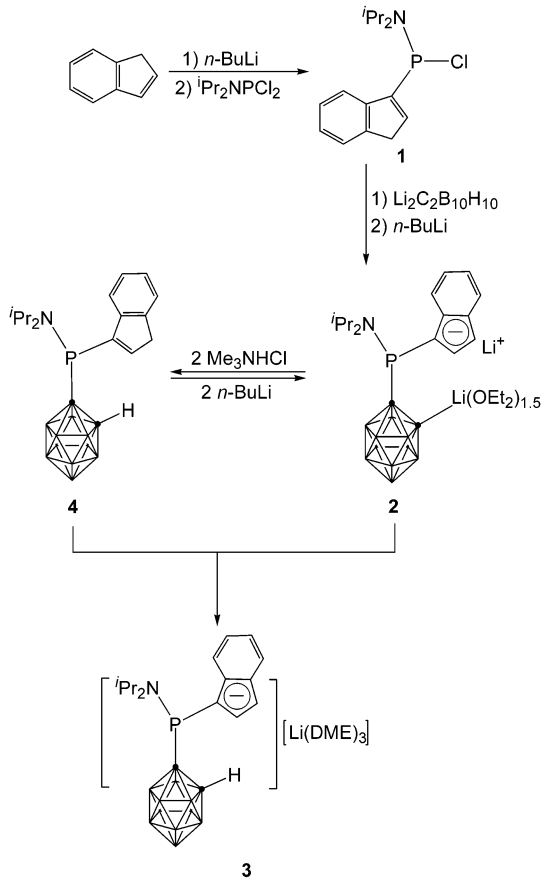

Compounds **1**−**4** were fully characterized by various spectroscopic techniques and elemental analyses. The solid-state structures of **1**, **3**, and **4** were further confirmed by single-crystal X-ray analyses. The ^{31}P chemical shifts are 120.2 ppm in **1**, 40.8 ppm in **2**, 41.6 ppm in **3**, and 74.1 and 40.1 ppm in **4**, respectively. Therefore, ^{31}P NMR spectroscopy may serve as a probe to monitor the transformations shown in Scheme 1. The presence of two resonances observed in the ^{31}P NMR spectrum of **4** indicates that it is a mixture of allylic and vinylic isomers with a molar ratio of ca. 1:0.7. This phenomenon is commonly observed in indene derivatives,[15a] resulting in the complex ^{1}H and ^{13}C NMR spectra. Couplings between the phosphorus and carbon nuclei make the ^{13}C NMR spectra of **1**−**3** complicated yet interpretable. The ^{11}B NMR spectra exhibit 5:2:3, 2:3:5, and 3:1:1:2:1:2 splitting patterns for **2**−**4**, respectively. Their IR spectra show a characteristic B−H absorption at about 2570 cm^{-1}.

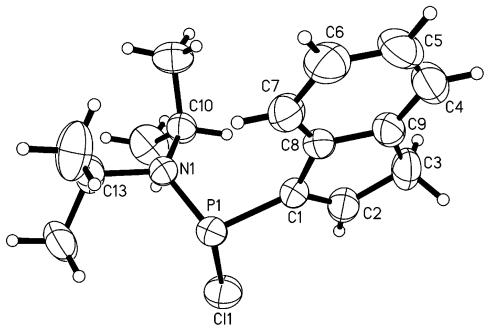

Figure 1. Molecular structure of ^{i}Pr$_2$NP(C$_9$H$_7$)Cl (**1**).

The molecular structure of **1** is shown in Figure 1. The C(1)−C(2) distance of 1.340(4) Å is indicative of a double bond, whereas the C(2)−C(3) and C(3)−C(9) distances are 1.509(5) and 1.498(5) Å, respectively. The C(2)−C(3)−C(9) angle is 102.5(3)°, which is the smallest one within the five-membered ring, as expected for an sp^3 carbon. The geometry of the nitrogen atom is close to a trigonal plane (the sum of angles around the N atom is 357.9°). However, the Cl−P(1)−C(1), C(1)−P(1)−N(1), and N(1)−P(1)−Cl angles (98.0(1), 102.9(1), and 105.6-

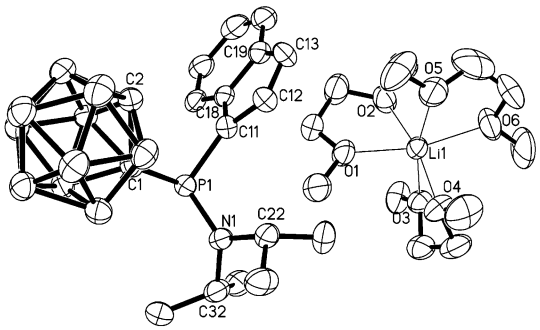

Figure 2. Molecular structure of $[^{i}Pr_2NP(C_9H_6)(C_2B_{10}H_{11})][Li(DME)_3]$ (**3**).

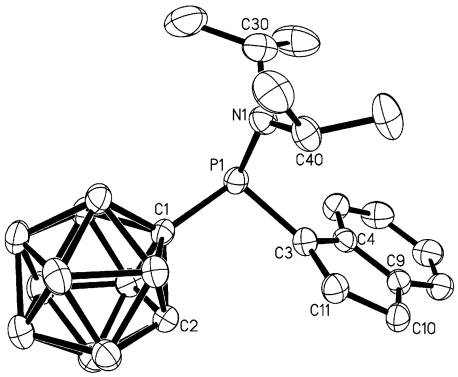

Figure 3. Molecular structure of $^{i}Pr_2NP(C_9H_7)(C_2B_{10}H_{11})$ (**4**).

(1)°) show that the coordination environment around phosphorus atom is trigonal pyramidal. These structural data suggest that the P atom is bonded to an sp^2 carbon in **1** and the presence of some N(pπ)−P(dπ) bond.[22,23]

An X-ray analysis reveals that the solid-state structure of **3** consists of well-separated, alternating layers of the discrete octahedral cations $[Li(DME)_3]^+$ and the trigonal-pyramidal anions $[^{i}Pr_2NP(C_9H_6)(C_2B_{10}H_{11})]^-$, shown in Figure 2. It indicates that DME can remove the Li^+ from the bonding with the indenyl group, leading to a naked anion. In the anion, the sum of angles around P and N atoms is 316.2 and 358.4°, respectively, indicating that the P atom still adopts a trigonal-pyramidal geometry and the presence of some N−P π bond. The P(1)−C(11) distance of 1.768(2) Å is significantly shorter than that of 1.820(3) Å observed in its parent compound **1**, probably suggesting the presence of some C−P π bond.

An X-ray analysis of **4** shows that it crystallizes in the form of a vinylic isomer (Figure 3). The structural data listed in Table 3 indicate that the geometry of both N and P atoms in **4** is very close to that in **3**, and the P atom is bonded to the sp^2 C of the indenyl group. The P−N and P−C(cage) distances in **4** are very close to the corresponding values in **3**. The P−C(ring) distance of 1.827(3) Å in **4** is significantly longer than that of 1.768(2) Å in **3** but is almost identical with that of 1.820(3) Å in **1**.

$[\eta^5$:σ-$^{i}Pr_2NP(C_9H_6)(C_2B_{10}H_{10})]Yb(DME)_2$ and $[\{\eta^5$:σ-$^{i}Pr_2NP(C_9H_6)(C_2B_{10}H_{10})\}_2Ln][Li(solvent)_n]$. Treatment of $YbI_2(THF)_x$ with 1 equiv of **2** in THF afforded,

Scheme 2

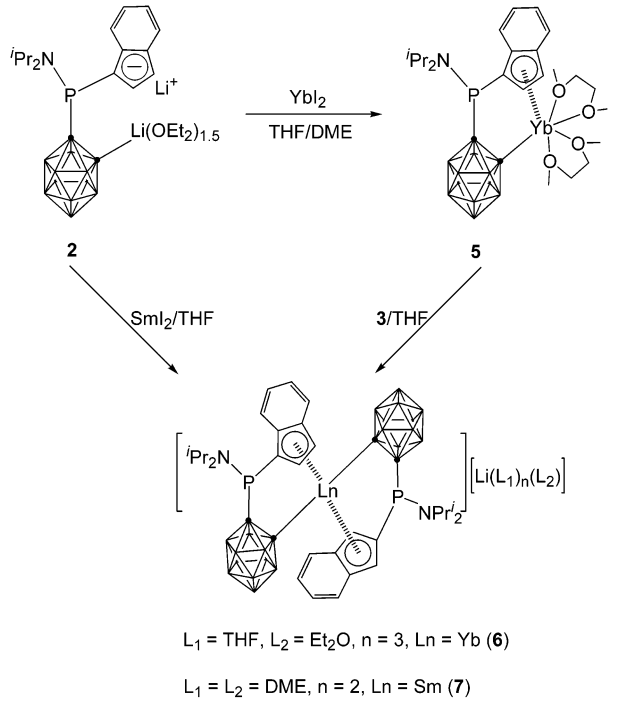

after recrystallization from a mixed solvent of DME and toluene, the orange-red organoytterbium(II) complex $[\eta^5$:σ-$^{i}Pr_2NP(C_9H_6)(C_2B_{10}H_{10})]Yb(DME)_2$ (**5**). **5** reacted with 1 equiv of **3** at room temperature to give the organoytterbium(III) complex $[\{\eta^5$:σ-$^{i}Pr_2NP(C_9H_6)(C_2B_{10}H_{10})\}_2Yb][Li(THF)_3(Et_2O)]$ (**6**). Apparently, the cage C−H bond is reduced by the Yb(II) species during the reaction, a phenomenon that was observed earlier in the Me_2C-bridged system.[6] This result suggests that **5** resembles $[\eta^5$:σ-$Me_2C(C_9H_6)(C_2B_{10}H_{10})]Yb(DME)_2$ in reactivity.

In sharp contrast, reaction of $SmI_2(THF)_x$ with 1 equiv of **2** in THF gave, after recrystallization from a mixed solution of DME and toluene, the trivalent samarium complex $[\{\eta^5$:σ-$^{i}Pr_2NP(C_9H_6)(C_2B_{10}H_{10})\}_2Sm][Li(DME)_3]$ (**7**) in 36% yield. No organosamarium(II) species was isolated. This result is similar to that reported for the reaction of $[Me_2A(C_9H_6)(C_2B_{10}H_{10})]Li_2$ (A = C, Si) with SmI_2.[6,7a] These transformations are summarized in Scheme 2.

Complex **7** and its analogues were also prepared using $LnCl_3$ as starting materials. Interactions between $LnCl_3$ and 2 equiv of **2** in THF gave, after recrystallization from the different solvent mixtures, the trivalent organolanthanide complexes $[\{\eta^5$:σ-$^{i}Pr_2NP(C_9H_6)(C_2B_{10}H_{10})\}_2Ln][Li(L_1)_nL_2]$ ($L_1 = L_2$ = DME, $n = 2$, Ln = Sm (**7**), Nd (**8**), Er (**9**); L_1 = DME, L_2 = THF, $n = 2$, Ln = Y (**10**)) (Scheme 3) in 42−69% yields.

Complexes **5**−**10** are soluble in polar organic solvents such as THF, DME, and pyridine, slightly soluble in toluene, and insoluble in *n*-hexane. The ^{31}P chemical shifts are 35.5 ppm for **5**, 42.9 ppm for **6**, 47.1 and 44.6 ppm for **7**, 44.1 and 32.5 ppm for **8**, 45.9 ppm for **9**, and 33.0 ppm for **10**, respectively. It is noteworthy that the ^{31}P NMR spectra of both **7** and **8** exhibit two resonances with the same intensity, which are presumably due to the relatively larger ionic radii of Sm^{3+} and Nd^{3+}, leading to a racemic−meso epimerization in solution.[6] This interconversion is probably prevented in the heavier

(22) Trinquier, G.; Ashby, M. T. *Inorg. Chem.* **1994**, *33*, 1306.
(23) Schick, G.; Loew, A.; Nieger, M.; Airola, K.; Niecke, E. *Chem. Ber.* **1996**, *129*, 911.

Scheme 3

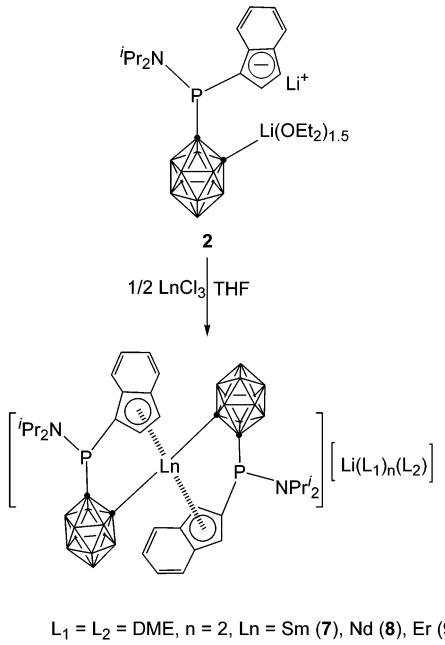

L$_1$ = L$_2$ = DME, n = 2, Ln = Sm (**7**), Nd (**8**), Er (**9**)

L$_1$ = DME, L$_2$ = THF, n = 2, Ln = Y (**10**)

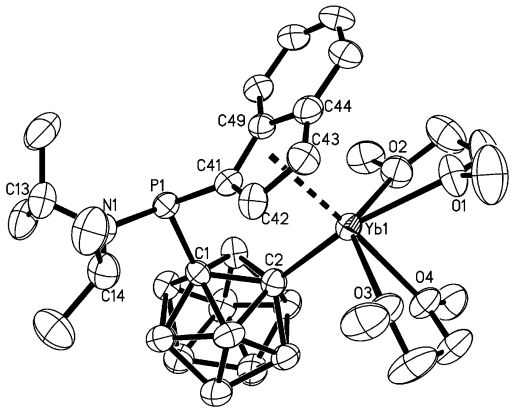

Figure 4. Molecular structure of [η^5:σ-^{i}Pr$_2$NP(C$_9$H$_6$)(C$_2$B$_{10}$H$_{10}$)]Yb(DME)$_2$ (**5**).

lanthanides because of the very crowded coordination environments.

Complexes **6**−**9** are paramagnetic species and do not offer useful ^{1}H and ^{13}C NMR information. For the diamagnetic yttrium complex **10**, the ^{1}H NMR spectrum exhibits four singlets of equal intensity for the methyl protons of −NCH(C*H*$_3$)$_2$. In addition, six multiplets in the aromatic region and a broad multiplet at δ 4.38 ppm were observed in the ^{1}H NMR, which are attributable to the indenyl protons and −CH− in NC*H*(CH$_3$)$_2$ groups, respectively. The broadening peaks are presumably caused by a longer range of P−H coupling. The resonances at δ 133.2 and 89.9 ppm with a large one-bond coupling to phosphorus ($^1J_{PC}$ = 45.7 and 60.7 Hz, respectively) observed in the ^{13}C NMR are assignable to the indenyl and cage carbon atoms that directly bond to the phosphorus atom.

The molecular structure of **5** is shown in Figure 4. The Yb atom is η^5-bound to the five-membered ring of the indenyl group, σ-bound to the carborane cage carbon atom, and coordinated to four oxygen atoms from two DME molecules in a distorted-octahedral geometry with

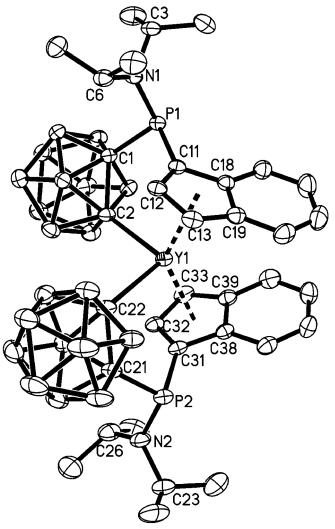

Figure 5. Molecular structure of the anion [{η^5:σ-^{i}Pr$_2$NP(C$_9$H$_6$)(C$_2$B$_{10}$H$_{10}$)}$_2$Y]$^-$ in **10**.

a formal coordination number of 8, which is similar to situation in the eight-coordinate [η^5:σ-Me$_2$C(C$_9$H$_6$)(C$_2$B$_{10}$H$_{10}$)]Yb(DME)$_2$.[6] The average Yb−C(C$_5$ ring) distance of 2.790(8) Å, the average Yb−O distance of 2.494(6) Å, and the Yb−C(cage) distance of 2.587(7) Å are comparable to the corresponding values of 2.789(8), 2.445(5), and 2.561(6) Å observed in [η^5:σ-Me$_2$C(C$_9$H$_6$)(C$_2$B$_{10}$H$_{10}$)]Yb(DME)$_2$.[6] The C(cage)−Yb−Cent (the centroid of the five-membered ring of indenyl) angle of 98.9° is significantly larger than that of 90.6° in [η^5:σ-Me$_2$C(C$_9$H$_6$)(C$_2$B$_{10}$H$_{10}$)]Yb(DME)$_2$[6] because of the difference in the sizes of the P and C atoms.

The solid-state structures of **6**−**8** and **10** as derived from single-crystal X-ray diffraction studies confirm that they consist of well-separated, alternating layers of discrete tetrahedral anions [{η^5:σ-^{i}Pr$_2$NP(C$_9$H$_6$)(C$_2$B$_{10}$H$_{10}$)}$_2$Ln]$^-$ and cations [Li(solvent)$_n$]$^+$. In the anions, the Ln^{3+} ion is η^5-bound to each of the two indenyl groups and σ-bound to two cage carbon atoms from two carboranyl moieties in a distorted-tetrahedral geometry. However, the orientation of the indenyl moieties in **10** is different from that observed in **6**−**8**. The former is a meso isomer, as shown in Figure 5, whereas the latter species are neither meso nor racemic isomers. A representative structure of the anions in **6**−**8** is shown in Figure 6. Such an orientation may result from steric effects and the rigidity of the linked ligand.

The geometries of the N and P atoms in **6**−**8**, **10**, and **3** are almost identical (Tables 3 and 4), showing that the geometry around the P atoms remains unchanged after complexation with lanthanides. The P−C(ring) distances are almost the same in all complexes, which are slightly longer than the corresponding value of 1.828(7) Å observed in [PhP(η^5-C$_5$Me$_4$)$_2$]ZrCl$_2$.[14g] The average Ln−C(cage) and Ln−C(ring) distances are very close to the corresponding values found in [η^5:σ-Me$_2$A(C$_9$H$_6$)(C$_2$B$_{10}$H$_{10}$)]$_2$Ln$^-$ (A = Si, C)[6,7] and [η^5:σ-^{i}Pr$_2$NB(C$_9$H$_6$)(C$_2$B$_{10}$H$_{10}$)$_2$Ln]$^-$,[10] respectively. Table 5 lists some structural parameters for the [η^5:σ-A(C$_9$H$_6$)(C$_2$B$_{10}$H$_{10}$)]$_2$-Ln$^-$ moieties. As the size of the bridging atom increases, the α angle decreases accordingly. However, the trend for the change of β angles is not very obvious.

[{[η^5:σ-^{i}Pr$_2$NP(C$_9$H$_6$)(C$_2$B$_{10}$H$_{10}$)]LnCl}$_2$(μ-Cl)$_3$Li(DME)][Li(DME)$_3$]$_2$. Lanthanocene chlorides are im-

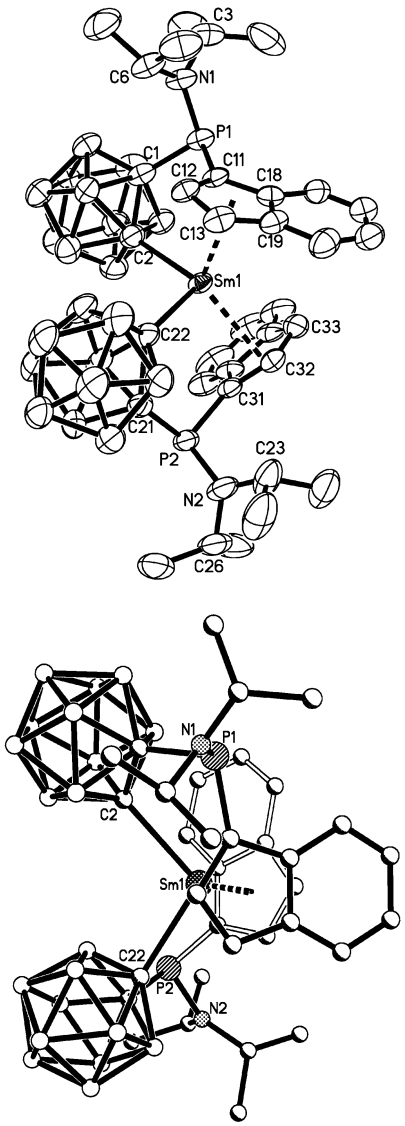

Figure 6. Molecular structure of the anion $[\{\eta^5{:}\sigma\text{-}^i\mathrm{Pr_2NP}(\mathrm{C_9H_6})(\mathrm{C_2B_{10}H_{10}})\}_2\mathrm{Sm}]^-$ in **7**: perspective view (top) and projective view (bottom).

Table 5. Structural Data (deg) for $[\eta^5{:}\sigma\text{-A}(\mathrm{C_9H_6})(\mathrm{C_2B_{10}H_{10}})]_2\mathrm{Ln}^-$

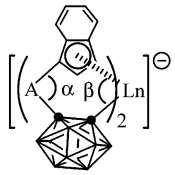

	Sm		Yb		
A	α	β	α	β	ref
$^i\mathrm{Pr_2NB}$	115.9	95.4	114.5	98.3	10
$\mathrm{Me_2C}$	111.4	93.3	111.2	97.2	6
$\mathrm{Me_2Si}$	108.1	102.5			7a
$^i\mathrm{Pr_2NP}$	101.2	97.5	99.7	101.6	this work

portant intermediates for the preparation of Ln−C- and Ln−heteroatom-containing organolanthanide compounds.[24] Our previous work shows that $[\mathrm{Me_2A}(\mathrm{C_9H_6})(\mathrm{C_2B_{10}H_{10}})]^{2-}$ (A = C,[6] Si[7a]) and $[^i\mathrm{Pr_2NB}(\mathrm{C_9H_6})(\mathrm{C_2B_{10}H_{10}})]^{2-}$ ligands[10] cannot stabilize lanthanocene chlorides, and only $[\{\eta^5{:}\sigma\text{-L}(\mathrm{C_9H_6})(\mathrm{C_2B_{10}H_{10}})\}_2\mathrm{Ln}]^-$ types of complexes (L = $\mathrm{Me_2C}$, $\mathrm{Me_2Si}$, $^i\mathrm{Pr_2NB}$) were isolated, regardless of the molar ratios of the reactants and the sizes of the lanthanides. It is of interest to compare the properties among these known ligands and the present one. Treatment of $\mathrm{LnCl_3}$ with 1 equiv of **2** in THF gave, after recrystallization from a mixed solvent of DME and toluene, the dimeric organolanthanide chloride complexes of the general formula $[\{[\eta^5{:}\sigma\text{-}^i\mathrm{Pr_2NP}(\mathrm{C_9H_6})(\mathrm{C_2B_{10}H_{10}})]\mathrm{LnCl}\}_2(\mu\text{-Cl})_3\mathrm{Li(DME)}][\mathrm{Li(DME)_3}]_2$ (Ln = Er (**11**), Y (**12**)) in moderate yields (Scheme 4). These results indicate that the present ligand can effectively prevent the half-sandwich organolanthanide chloride complexes from the ligand redistribution reactions, which differ significantly from the $\mathrm{Me_2C}$-, $\mathrm{Me_2Si}$-, and $^i\mathrm{Pr_2NB}$-bridged analogues. The paramagnetic complex **11** does not offer useful NMR information. However, the diamagnetic yttrium complex **12** provides interpretable NMR data. Its ^{1}H and ^{13}C NMR spectra are very similar to those of complex **10**. On the other hand, the ^{11}B NMR is different from that of **10**, showing a 1:2:2:1:1:2:1 splitting pattern. A downfield-shifted ^{31}P NMR signal (δ 45.6 ppm) was observed in **12**, in comparison with that (δ 33.0 ppm) of **10**.

Scheme 4

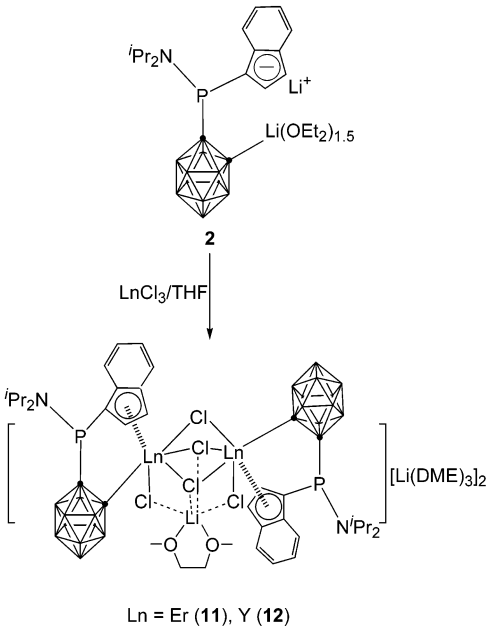

Ln = Er (**11**), Y (**12**)

The molecular structures of **11** and **12** were confirmed by X-ray analyses. They are isomorphous and isostructural, consisting of the octahedral cations $[\mathrm{Li(DME)_3}]^+$ and the complex anions $[\{[\eta^5{:}\sigma\text{-}^i\mathrm{Pr_2NP}(\mathrm{C_9H_6})(\mathrm{C_2B_{10}H_{10}})]\mathrm{LnCl}\}_2(\mu\text{-Cl})_3\mathrm{Li(DME)}]^{2-}$. Figure 7 shows the representative structure of the anion in **11**. In the anion, each $\mathrm{Ln^{3+}}$ ion is η^5-bound to one five-membered ring of the indenyl group and σ-bound to one cage carbon atom, two doubly bridging Cl atoms, and two triply bridging Cl atoms in a distorted-octahedral arrangement. In comparison with $[\{\eta^5{:}\sigma\text{-}\mathrm{Me_2Si}(\mathrm{C_5Me_4})(\mathrm{C_2B_{10}H_{10}})\}\mathrm{YbCl}(\mu\text{-Cl})][\mathrm{Li(DME)_3}]_2$,[5a] the presence of the additional bridging Cl atoms in **11** and **12** is presumably due to the higher Lewis acidity of the central metal ions, resulting from

(24) For reviews, see: (a) Schumann, H.; Messe-Markscheffel, J. A.; Esser, L. *Chem. Rev.* **1995**, *95*, 865. (b) Edelmann, F. T. In *Comprehensive Organometallic Chemistry II*; Abel, E. W., Stone, F. G. A., Wilkinson, G., Eds.; Pergamon: New York, 1995; Vol. 4, p 11.

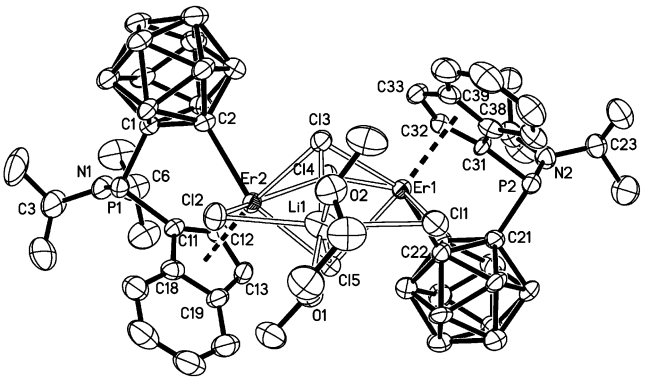

Figure 7. Molecular structure of the anion $[\{[\eta^5{:}\sigma\text{-}^i\mathrm{Pr}_2\mathrm{NP}(\mathrm{C_9H_6})(\mathrm{C_2B_{10}H_{10}})]\mathrm{ErCl}\}_2(\mu\text{-Cl})_3\mathrm{Li(DME)}]^{2-}$ in **11**.

the poorer electron-donating ability of the indenyl group compared with that of the tetramethylcyclopentadienyl group.

Reactivity. Complexes **11** and **12** represent the very rare structurally characterized examples of organolanthanide compounds bearing both Ln−C π and σ bonds as well as a Ln−Cl σ bond.[24] The chlorine atoms in these lanthanocene chlorides are expected to be replaced by other groups via salt metathesis reactions. In fact, treatment of **12** with 2 equiv of KCH_2Ph in THF afforded, after recrystallization from toluene, the unexpected product $\{[\eta^5{:}\sigma\text{-}^i\mathrm{Pr}_2\mathrm{NP}(\mathrm{C_9H_6})(\mathrm{C_2B_{10}H_{10}})]_2\mathrm{Y}\}\{(\eta^6\text{-}\mathrm{C_6H_5CH_3})_2\mathrm{K}\}$ (**13**) in 57% yield (Scheme 5). The expected complex $[\eta^5{:}\sigma\text{-}^i\mathrm{Pr}_2\mathrm{NP}(\mathrm{C_9H_6})(\mathrm{C_2B_{10}H_{10}})]\mathrm{YCH_2Ph(solvent)}_n$ was not isolated, but it may serve as an intermediate. This highly coordinatively unsaturated species may undergo a ligand redistribution reaction to generate the thermodynamically more stable complex **13**. We then turned to the sterically more demanding reagent $\mathrm{LiN(SiMe_3)_2}$ in the hope of preparing a complex containing Ln−C π and σ bonds as well as an Ln−N bond.

Reaction of **12** with 2 equiv of $\mathrm{LiN(SiMe_3)_2}$ in THF gave, after recrystallization from DME/THF, the ionic complex $[\{\eta^5{:}\sigma\text{-}^i\mathrm{Pr}_2\mathrm{NP}(\mathrm{C_9H_6})(\mathrm{C_2B_{10}H_{10}})\}_2\mathrm{Y}][\mathrm{Li(DME)_2(THF)}]$ (**10**). Apparently, $\mathrm{N(SiMe_3)_2^-}$ cannot prevent the ligand redistribution reaction. Reactions of **12** with alkylating reagents such as CH_3Li, Me_3SiCH_2M (M = Li, K), and Me_3SiCH_2MgCl were complicated, and no pure products were isolated. These results suggest that monodentate ligands may not be able to stabilize the desirable products. Multidentate ligands were then examined.

Treatment of **12** with 2 equiv of $NaBH_4$ in THF produced the expected complex $[\{\eta^5{:}\sigma\text{-}^i\mathrm{Pr}_2\mathrm{NP}(\mathrm{C_9H_6})(\mathrm{C_2B_{10}H_{10}})\}\mathrm{Y}\{(\mu\text{-H})_3\mathrm{BH}\}_2][\mathrm{Li(DME)_3}]$ (**14**) in 65% yield (Scheme 5). The successful isolation of **14** supports the previously proposed reaction pathway for the reactions of **12** with KCH_2Ph and $\mathrm{LiN(SiMe_3)_2}$.

It has been documented that lanthanocenes can be efficiently prepared via silylamine elimination reactions of $\mathrm{Ln[N(SiHMe_2)_2]_3(THF)_2}$ with protic reagents[25] or through alkane elimination reactions of $\mathrm{Ln(CH_2SiMe_3)_3(THF)_2}$ with protic reagents.[26] Compound **4** possesses two acidic protons, which may allow similar silylamine or alkane elimination reactions to occur. Equimolar reactions between **4** and $\mathrm{Ln[N(SiHMe_2)_2]_3(THF)_2}$ or $\mathrm{Ln(CH_2SiMe_3)_3(THF)_2}$ (Ln = Y, Er) in toluene or toluene/DME were attempted. These reactions were followed by both ^{31}P and ^{11}B NMR spectroscopy. To our surprise, there were no reactions at all at temperatures of 0−60 °C. As the temperature was increased to >60 °C, the color of the mixture changed from pale yellow (Ln = Y) or pink (Ln = Er) to red and finally to dark red. Many ^{31}P peaks appeared, suggesting that complicated reactions proceeded at temperatures >60 °C. These results imply that acidity/basicity is not the sole factor controlling these elimination reactions; steric factors must be taken into account.

Scheme 5

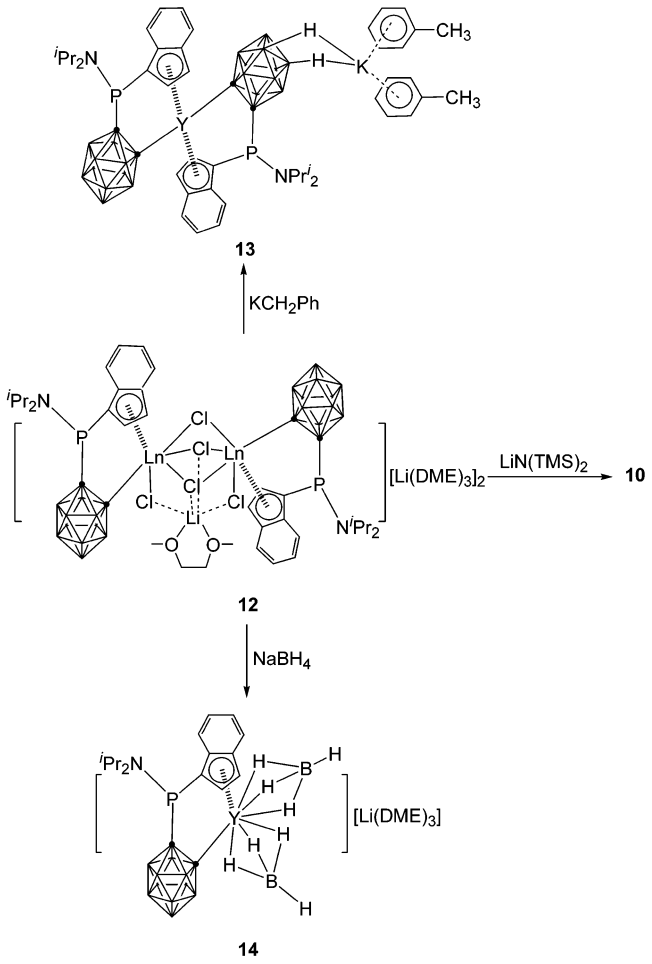

Both complexes **13** and **14** were confirmed by various spectroscopic data, elemental analyses, and single-crystal X-ray analyses. The ^1H NMR spectra support the ratio of one toluene molecule per indenyl−carboranyl ligand in **13** and three DME molecules per ligand in **14**. The ^{11}B NMR spectra show a 3:2 splitting pattern for **13** and a 2:1:3:4:2 splitting pattern for **14**. In addition, a resonance at −30.8 ppm that is assignable

(25) Eppinger, J.; Spiegler, M.; Hieringer, W.; Herrmann, W. A.; Anwander, R. *J. Am. Chem. Soc.* **2000**, *122*, 3080.

(26) (a) Lee, L.; Berg, D. J.; Bushnell, G. W. *Organometallics* **1995**, *14*, 8. (b) Lee, L.; Berg, D. J.; Einstein, F. W.; Batchelor, R. J. *Organometallics* **1997**, *16*, 1819. (c) Mu, Y.; Piers, W. E.; MacQuarrie, D. C.; Zaworotko, M. J.; Young, V. G., Jr. *Organometallics* **1996**, *15*, 2720. (d) Kirillov, E.; Toupet, L.; Lehmann, C. W.; Razavi, A.; Carpentier, J.-F. *Organometallics* **2003**, *22*, 4467.

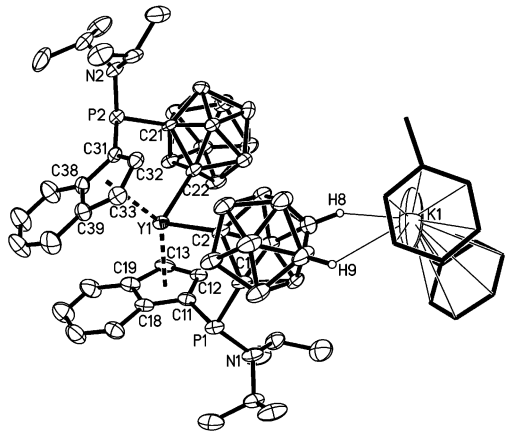

Figure 8. 8. Molecular structure of $\{[\eta^5{:}\sigma\text{-}^i\mathrm{Pr}_2\mathrm{NP}(\mathrm{C}_9\mathrm{H}_6)(\mathrm{C}_2\mathrm{B}_{10}\mathrm{H}_{10})]_2\mathrm{Y}\}\{[\eta^6\text{-}\mathrm{C}_6\mathrm{H}_5\mathrm{CH}_3]_2\mathrm{K}\}$ (**13**).

to BH_4^- was also observed in the ^{11}B NMR spectrum of **14**. The ^{31}P chemical shifts are 41.2 ppm for **13** and 42.8 ppm for **14**, respectively.

An X-ray diffraction study reveals that **13** is composed of the cation $[K(CH_3Ph)_2]^+$ and the anion $[\{\eta^5{:}\sigma\text{-}^i\mathrm{Pr}_2\mathrm{NP}(\mathrm{C}_9\mathrm{H}_6)(\mathrm{C}_2\mathrm{B}_{10}\mathrm{H}_{10})\}_2\mathrm{Y}]^-$, which are connected each other through two B−H−K interactions, as shown in Figure 8. The geometry of the anion is almost identical with that in **10**. The K^+ ion is asymmetrically bonded to two toluene molecules in a η^6-fashion. The K···H−B (3.387(5) Å) and K···C (3.340(5) Å) distances are comparable to the literature data.[27]

The molecular structure of **14** is shown in Figure 9. As indicated in Table 4, the geometry of the $[\eta^5{:}\sigma\text{-}^i\mathrm{Pr}_2\mathrm{NP}(\mathrm{C}_9\mathrm{H}_6)(\mathrm{C}_2\mathrm{B}_{10}\mathrm{H}_{10})]\mathrm{Y}^+$ fragment is similar to that observed in its parent complex **12**. The bonding mode of the BH_4^- group may be determined according to the Y−B distances. For η^2-BH_4^-, the Y−B distances are normally in the range 2.68−2.77 Å.[28] These distances are significantly shortened for the metal complexes bearing tridentate coordination of the BH_4^- groups: for instance, 2.58(1) Å in $Y(BH_4)_3(THF)_3$.[28d] The Y−B distances (2.485(3) and 2.499(3) Å) observed in **14** are the shortest ones among literature data. It is therefore

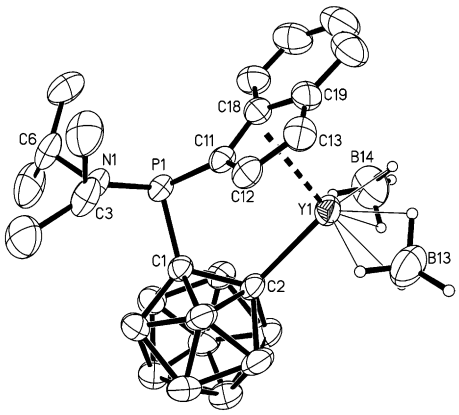

Figure 9. Molecular structure of the anion $[\{\eta^5{:}\sigma\text{-}^i\mathrm{Pr}_2\mathrm{NP}(\mathrm{C}_9\mathrm{H}_6)(\mathrm{C}_2\mathrm{B}_{10}\mathrm{H}_{10})\}\mathrm{Y}\{(\mu\text{-}\mathrm{H})_3\mathrm{BH}\}_2]^-$ in **14**.

suggested that both BH_4^- groups in **14** adopt a tridentate coordination mode.

Conclusions

A new phosphorus-bridged indenyl−carboranyl (organic−inorganic) hybrid ligand was designed and successfully prepared. Several tri- and divalent organolanthanide complexes derived from this ligand were synthesized and fully characterized. Experimental results show that $^i\mathrm{Pr}_2\mathrm{NP}(\mathrm{C}_9\mathrm{H}_7)(\mathrm{C}_2\mathrm{B}_{10}\mathrm{H}_{11})$ possesses not only the common features exhibited by its close relatives such as $\mathrm{Me}_2\mathrm{C}(\mathrm{C}_9\mathrm{H}_7)(\mathrm{C}_2\mathrm{B}_{10}\mathrm{H}_{11})$,[6a] $\mathrm{Me}_2\mathrm{Si}(\mathrm{C}_9\mathrm{H}_7)(\mathrm{C}_2\mathrm{B}_{10}\mathrm{H}_{11})$,[7] and $^i\mathrm{Pr}_2\mathrm{NB}(\mathrm{C}_9\mathrm{H}_7)(\mathrm{C}_2\mathrm{B}_{10}\mathrm{H}_{11})$[10] but also unique properties of its own. For example, it can effectively stabilize lanthanocene chlorides, and the phosphorus atom always adopts a trigonal-pyramidal geometry with an electron pair available for possible bonding.

Acknowledgment. The work described in this paper was supported by a grant from the Research Grants Council of the Hong Kong Special Administration Region (Project No. CUHK4026/02P). Z.X. acknowledges the Croucher Foundation for a Senior Research Fellowship Award.

Supporting Information Available: Crystallographic data and data collection details, atomic coordinates, bond distances and angles, anisotropic thermal parameters, and hydrogen atom coordinates for complexes **1**, **3**−**8**, and **10**−**14** as CIF files. This material is available free of charge via the Internet at http:/pubs.acs.org.

OM034268L

(27) Chui, K.; Li, H.-W.; Xie, Z. *Organometallics* **2000**, *19*, 5447.

(28) (a) Qian, C.; Zou, G.; Nie, W.-Li.; Sun, J.; Lemenovskil, D. A.; Borzov, M. V. *Polyhedron* **2000**, *19*, 1955. (b) Deng, D.; Zhang, X.; Qian, C.; Sun, J.; Zhang, L. *J. Organomet. Chem*. **1994**, *466*, 95. (c) Laske, D. A.; Duchateau, R.; Teuben, J. H. *J. Organomet. Chem*. **1993**, *462*, 149. (d) Deng, D.; Zheng, X. Qian, C. *Acta Chim. Sin*. **1992**, *50*, 1024. (e) Segal, B.; Lippard, S. J. *Inorg. Chem*. **1978**, *17*, 844.